Scientific Research Publishing

World Journal of Engineering and Technology, 2024, 12, 103-116
https://www.scirp.org/journal/wjet
ISSN Online: 2331-4249
ISSN Print: 2331-4222

Stability Analysis of Nonlinear Models of Nose Landing Gear Shimmy

Jiacai Zhou, Yanying Zhao*, Qiqi Li, Longhua Zhou

School of Aircraft Engineering, Nanchang Hangkong University, Nanchang, China
Email: *yanyingzhao@nchu.edu.cn

How to cite this paper: Zhou, J.C., Zhao, Y.Y., Li, Q.Q. and Zhou, L.H. (2024) Stability Analysis of Nonlinear Models of Nose Landing Gear Shimmy. *World Journal of Engineering and Technology*, **12**, 103-116.
https://doi.org/10.4236/wjet.2024.121007

Received: January 23, 2024
Accepted: February 3, 2024
Published: February 6, 2024

Abstract

Shimmy can reduce the service life of the nose landing gear, affect ride comfort, and even cause fuselage damage leading to aircraft crashes. Taking a light aircraft as the research object, the torsional freedom of landing gear around strut axis and lateral deformation of tire are considered. Since the landing gear shimmy is a nonlinear system, a nonlinear mechanical model of the front landing gear shimmy is established. Sobol index method is proposed to analyze the influence of structural parameters on the stability region of the nose landing gear, and Routh-Huritz criterion is used to verify the reliability of the analysis results of Sobol index method. We analyse the effect of torsional stiffness of strut, caster length, rated initial tire inflation pressure, rake angle, and vertical force on the stability region of theront landing gear. And the research shows that the optimization of the torsional stiffness of the strut and the caster length of the nose landing gear should be emphasized, and the influence of vertical force on the stability region of the nose landing gear should be paid attention to.

Keywords

Nose Landing Gear, Shimmy Oscillations, Stability, Sobol Index Method

1. Introduction

The landing gear is suddenly excited by external excitation, which will produce certain deformation and torsion angle. When the external excitation disappears, the self-excited nonlinear instability phenomenon of the wheel torsion around the landing gear strut axis is called landing gear shimmy.

In the middle of the last century, Moreland [1] and Smiley [2] proposed the Point Contact Theory and Stretched String Theory with different assumptions based on tyre deformation. After a lot of theoretical analysis and experimental

research, the two theories have been widely recognized and used. Boeckh [3] had measured the deformation of four different tires through experiments, and obtained the rotational inertia of the tire around the vertical axis and verified the Stretched String model. Besselink *et al.* [4] thought that with the change of motion state, the motion characteristics of tires would also change, and it changed greatly. Thota *et al.* [5] studied the relationship between the nose landing gear shimmy oscillation characteristics of passenger aircraft and tire inflation pressure, also conducting a bifurcation analysis of landing gear shimmy oscillation, then obtained two-parameter bifurcation diagrams for five different inflation pressures, which showed that the landing gear is not susceptible to shimmy oscillation at higher than nominal inflation pressure. Ran *et al.* [6] introduced the Tyre models with the Magic Formula and a non-constant relaxation length, and compared the two tire models using the energy flow method. The results show that the shimmy model with non-constant relaxation length tire model can obtain more accurate results when the amplitude is large.

Analysis of landing gear shimmy frequency domain is an important theme of landing gear shimmy. Sateesh *et al.* [7] pointed out that runway excitation leads to a significant reduction in the critical shimmy speed of the landing gear. The interaction of runway roughness and landing gear torsional free play adversely affects the lateral stability of the landing gear. Sura *et al.* [8] established a three-degree-of-freedom nose wheel landing gear shimmy model, and obtained the analytical expressions of shimmy velocity and shimmy frequency (shimmy instability), the shimmy frequency approximates the lowest natural frequency of the nose landing gear on the ground. Chuban [9] used the finite element method to obtain the natural frequencies and modes of landing gear shimmy.

In academic circles landing gear shimmy is generally considered to be a shimmy problem consisting of multiple degrees of freedom coupled together by tire deformation, strut torsional deformation and strut lateral deformation. Somieski [10] established a two-degree-of-freedom shimmy dynamics model for the nose landing gear and analyzed the stability problem of shimmy. Thota *et al.* [11] has established a three-degree-of-freedom shimmy dynamics model of the nose landing gear. The three degrees of freedom are the lateral bending of the strut, the torsion of the strut and the lateral deformation of the tire. The bifurcation analysis of the landing gear shimmy is carried out using the numerical continuation method, and the shimmy stability region was analyzed. Thota *et al.* [12] added the longitudinal bending of the strut on the basis of his existing research, and concluded that the longitudinal bending of the strut has very little impact on the stability area of the landing gear shimmy. Rahmani *et al.* [13] divided the torsion of the strut into three degrees of freedom (the lower strut rotates around the strut axis, the upper strut rotates around the strut axis, and the shimmy damper rotates around the strut axis) for analysis. Through analysis, it was found that smaller stiffness and larger damping of the shimmy damper can improve the performance of the shimmy damper.

With the in-depth study of landing gear oscillation, it is found that many de-

tails cannot be ignored. Collins *et al.* [14] divided the landing gear shimmy into "Tire-Yaw" shimmy and "Structural-Torsion" shimmy. Behdinani *et al.* [15] adopted the treatment method similar to that of Howcroft *et al.* [16] for the torque link apex freeplay, and established 1 the freeplay nose landing gear shimmy model including Coulomb friction factor. The results show that the stability of the nose landing gear system decreases with the increase of the freeplay. It is found that the increase of Coulomb friction factor will reduce the shimmy stability area dominated by torsion. Kewley *et al.* [17] added the lateral and vertical displacement of the fuselage on the basis of the model proposed by Thota *et al.* [18], representing the yaw of the fuselage on the runway and the pitch of the fuselage respectively. Jiang *et al.* [19] established a nonlinear dynamic model of nose landing gear shimmy coupled with time-varying load and Coulomb friction, and showed that the shimmy reduction effect of Coulomb friction is weakened under time-varying load.

The paper is structured as follows. Firstly, a mathematical model of nose landing gear shimmy is given and a sensitivity analysis of the nose landing gear structural parameters using Sobol's index is carried out in Section 2. The results of the Sobol index analysis are validated using Ross-Holwitz in Section 3. The conclusions are given in Section 4.

2. The Mathematical Model

A model diagram of a single-wheel nose landing gear for a light airplane is shown in **Figure 1**. The nose landing gear is a highly coupled nonlinear system, consisting mainly of strut sections, wheels, *et al.* The strut section consists of the upper strut and the lower strut, etc. (**Table 1**). The torque is transmitted through the upper and lower torque arms. This type of nose landing gear is from a light aircraft with retractable nose landing gear. It has a Caster length L, a Rake angle δ, and is taxiing on the runway at the same speed as the fuselage through wheels of radius R. The positive X-axis refers to the backward direction of the aircraft, the Y-axis has its positive direction determined by the right-hand coordinate system, and vertically up is the positive direction of the Z-axis.

In this paper, the nose landing gear shimmy is described by two degrees of freedom: the torsion angle (θ), which represents the rotation of the strut about its axis S, and the lateral deformation of the tire (Δ). It is assumed that the tires do not slip relative to the ground while the aircraft is taxiing on the runway without considering the effect of the fuselage on the front landing gear.

Because of the Rake angle δ, the swivel Angle ζ of the wheel is slightly lower than the torsion Angle (θ) of the nose landing gear strut, and its magnitude is equal to $\zeta = \theta\cos(\delta)$. The stretched string theory proposed by Von-Schlippe was adopted to simplify the tire model of the nose landing gear, as shown in **Figure 2**. The tyre will slip, when the lateral force exceeds a certain limit. The slip angle of each tyre is given by $\eta = \arctan(\Delta/\sigma) \approx \Delta/\sigma$.

Tire compression λ can be obtained from the following formula:

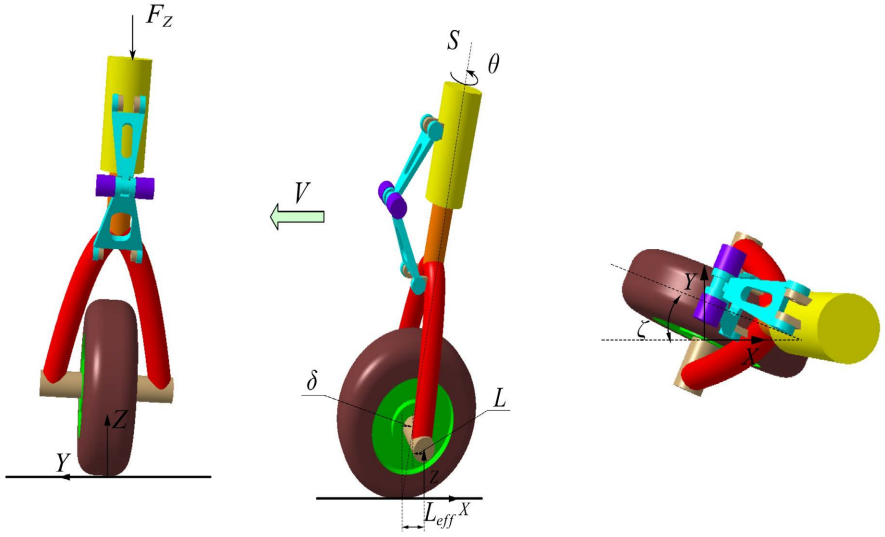

Figure 1. Schematic diagram of the single-wheel nose landing gear model.

Table 1. Structural parameters of the nose landing gear.

Symbols	Parameter	Value	Unit
Geometric parameters			
δ	Rake angle	0.1571	rad
L	Caster length	0.07	m
Strut parameters			
K_θ	Torsional stiffness of strut	10,000	N·m/rad
C_θ	Torsional damping of strut	10	N·m·s/rad
I_Z	Torsional inertia of strut	1	Kg·m^2
Wheel parameters			
D	Wheel diameter	0.3	m
W	Wheel width	0.125	m
P_0	Rated initial tire inflation pressure	600000	pa
P_r	Rated tire inflation pressure	600000	pa
C_{M_η}	Tire rotational stiffness coefficient	2	rad^{-1}
C_{F_η}	Tire lateral stiffness coefficient	20	m/rad
K	Tire rotational damping coefficient	270	N·m^2/rad
K_n	Tire lateral stiffness coefficient	2.8	rad^{-1}
η_m	self-aligning moment Limit side angle	0.1744	rad
η_F	Tire Lateral Force Limit side angle	0.0872	rad
external parameter			
F_Z	Vertical force	1800	N
V	velocity	0 - 100	m/s

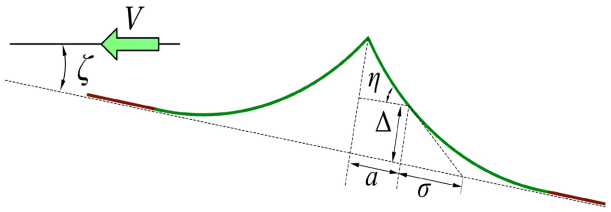

Figure 2. Tire mechanical model.

$$\lambda = \frac{F_Z}{2.4\left(P_0 + 0.08P_r\right)\sqrt{WD}} + 0.03W \tag{1}$$

Half of the Contact patch length a can be expressed by the amount of tire compression λ and the diameter of the wheel D:

$$a = 0.85D\sqrt{\frac{\lambda}{D} - \left(\frac{\lambda}{D}\right)^2} \tag{2}$$

P is the internal pressure of the tire when the corresponding compression amount is λ:

$$P = P_0 + 1.5\frac{W}{D}P_0\left(\frac{\lambda}{W}\right)^2 \tag{3}$$

Relaxation length σ is obtained from the following formula:

$$\sigma = \left(2.8 - 0.8\frac{P}{P_r}\right)\left(1 - 4.5\frac{\lambda}{D}\right)W \tag{4}$$

In summary, considering strut torsion and tire lateral deformation, the equation of nose landing gear nonlinear shimmy is given, as shown in Equation (5)-(6):

$$I_Z\ddot{\theta} + C_\theta\dot{\theta} + K_\theta\theta + M_F + M_D = 0 \tag{5}$$

$$\dot{\Delta} + V/\sigma\Delta - V\zeta - \left(L_{eff} - a\right)\dot{\zeta} = 0 \tag{6}$$

Because of the Rake angle δ, the effective Caster length L_{eff} is no longer equal to L, which is given by:

$$L_{eff} = L\cos(\delta) + \left(D/2 + L\sin(\delta)\right)\tan(\delta) \tag{7}$$

The typical changing tendency of the nonlinear restoring force of the tire F_n and self-aligning moment M_n with lateral deformation of the tire is shown in Figure 3. The combined moment M_F is generated by the self-aligning moment M_n and the nonlinear restoring force of the tire F_n, which equals to

$$M_F = \left(M_n + L_{eff}F_n\right)\cos(\delta) \tag{8}$$

$$F_n = K_n\tan^{-1}\left(7.0\tan(\eta)\right)\cos\left(0.95\tan^{-1}\left(7.0\tan(\eta)\right)\right)F_Z \tag{9}$$

$$M_n = \begin{cases} C_{M_\eta}F_Z\left(\dfrac{\eta_m}{180^\circ}\right)\sin\left(\dfrac{180^\circ}{\eta_m}\eta\right) & |\eta| \le \eta_m \\ 0 & |\eta| \ge \eta_m \end{cases} \tag{10}$$

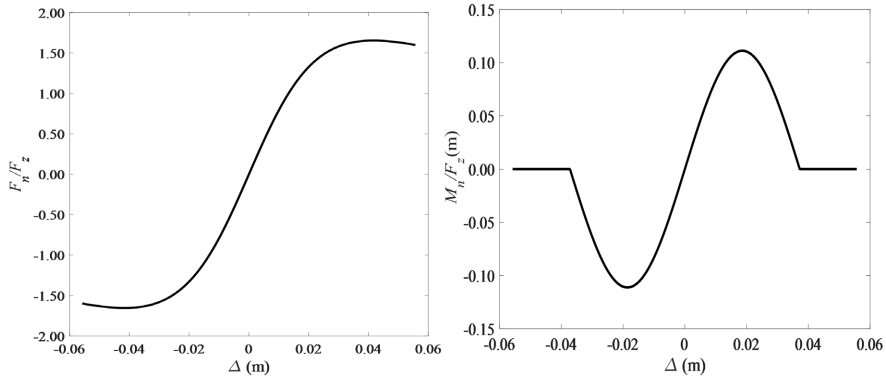

Figure 3. Nonlinear restoring force of the tire and self-aligning moment with different lateral deformation of the tire.

The moment M_D is generated by the tire tread damping and is given as

$$M_D = \frac{K}{V}\dot{\zeta} \tag{11}$$

3. Sensitivity Analysis of Structural Parameters

Sensitivity analysis is to determine the extent to which the parameters affect the model output, and provide a basis for the next model optimization, and also improve the efficiency of the optimization. Sensitivity analysis methods are divided into two categories: local sensitivity analysis and global sensitivity analysis. Local sensitivity is suitable for mathematical expressions that are relatively simple and easy to differentiate. Local sensitivity analyzes the effect of changes in only a single parameter on the system. Global sensitivity analysis can analyze the influence of a single parameter change on the model output, and can analyze the influence of multiple parameter interactions on the model output.

Due to the consideration of the nonlinear self-aligning moment and the restoring force of the tyre, the shimmy model is a system of nonlinear equations. At present, the critical velocity of shimmy cannot be given by the function analytical expression, but by numerical simulation (as shown in **Figure 4**). The number of structural parameters of the shimmy model is relatively large, and the global sensitivity analysis method is more suitable for the sensitivity analysis of this model than the local sensitivity analysis method. The Sobol index method in the global sensitivity analysis was chosen for comprehensive consideration; the sensitivity index cannot be calculated directly by the functional analysis method, but it can be calculated by the Monte Carlo method.

Structural parameter sensitivity analysis of the nose landing gear shimmy was performed, and the following structural parameters were selected: Torsional stiffness of strut, Caster length, Rated initial tire inflation pressure, Rake angle, and Vertical force. The range of values for each structural parameter is shown in **Table 2**.

For ease of representation, V_{cr} is simplified to V. The critical velocity of shimmy V is used as the output of the nose landing gear shimmy model:

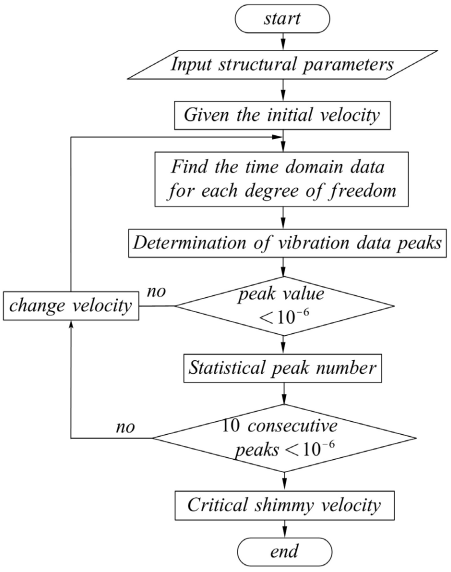

Figure 4. Critical velocity of shimmy flowchart.

Table 2. Range of values for relevant structural parameters.

Symbols	range of values	Unit
K_θ	[1000, 20,000]	N·m/rad
L	[0.001, 0.117]	m
P_0	[110,000, 1,200,000]	pa
δ	[0, 0.3]	rad
F_Z	[1510, 3600]	N

$$V = f(x) \tag{12}$$

Sampling is based on the range of the five independent variables described above (**Figure 5**), and the Sobol sequence sampling method is chosen for the sampling. This will generate a $n \times 2k$ sample matrix:

$$M = \begin{pmatrix} x_{11} & \cdots & x_{1k} & \cdots & x_{12k} \\ x_{21} & \cdots & x_{2k} & \cdots & x_{22k} \\ \vdots & & \vdots & & \vdots \\ x_{n1} & \cdots & x_{nk} & \cdots & x_{n2k} \end{pmatrix} \tag{13}$$

The first k columns of the extraction matrix M are set to the parameter matrix A, and the last k columns are set to the parameter matrix B:

$$A = \begin{pmatrix} x_{11} & x_{12} & \cdots & x_{1k} \\ x_{21} & x_{22} & \cdots & x_{2k} \\ \vdots & \vdots & & \vdots \\ x_{n1} & x_{n2} & \cdots & x_{nk} \end{pmatrix} \tag{14}$$

$$B = \begin{pmatrix} x_{1k+1} & x_{1k+2} & \cdots & x_{12k} \\ x_{2k+1} & x_{2k+2} & \cdots & x_{22k} \\ \vdots & \vdots & & \vdots \\ x_{nk+1} & x_{nk+2} & \cdots & x_{n2k} \end{pmatrix} \tag{15}$$

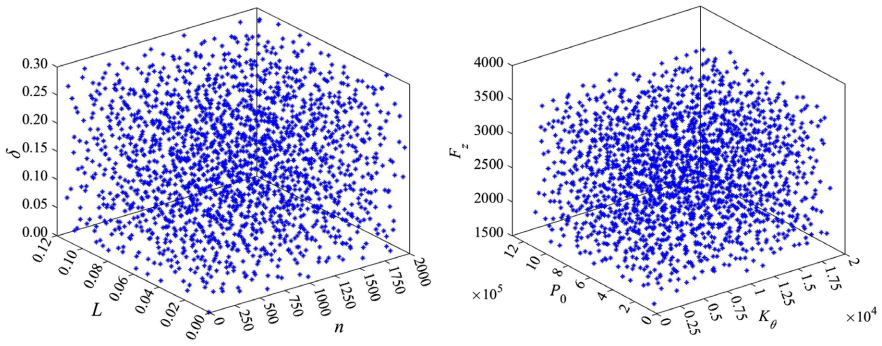

Figure 5. Sampling distribution for each structural parameter.

where: k is the number of covariates ($k=5$); n is the number of samples sampled ($n=2000$).

The new parameter matrix AB^i ($i=1,2,\cdots,k$) is obtained by replacing the ith column in matrix A with the value of the ith column of matrix B:

$$AB^i=\begin{pmatrix} x_{11} & x_{1k+i} & \cdots & x_{1k} \\ x_{21} & x_{2k+i} & \cdots & x_{2k} \\ \vdots & \vdots & & \vdots \\ x_{n1} & x_{nk+i} & \cdots & x_{nk} \end{pmatrix} \tag{16}$$

The parameter matrices A, B and AB^i are introduced into the pendulum oscillation model to obtain the system output vectors V_A、V_B and V_{AB^i} for each parameter matrix. According to the Monte Carlo method, the first order sensitivity (main effect) index S_{x_i} and the full effect index $S_{x_i}^T$ for each variable are denoted as

$$S_{x_i}=\frac{Var_{x_i}\left(E_{x_{-i}}\left(V\mid x_i\right)\right)}{Var\left(V\right)} \tag{17}$$

$$S_{x_i}^T=\frac{E_{x_{-i}}\left(Var_{x_i}\left(V\mid x_i\right)\right)}{Var\left(V\right)} \tag{18}$$

where $Var_{x_i}\left(E_{x_{-i}}\left(V\mid x_i\right)\right)$、$E_{x_{-i}}\left(Var_{x_i}\left(V\mid x_i\right)\right)$ and $Var\left(V\right)$ are respectively:

$$Var_{x_i}\left(E_{x_{-i}}\left(V\mid x_i\right)\right)\approx\frac{1}{n}V_B^T\left(V_{AB^i}-V_A\right)$$

$$E_{x_{-i}}\left(Var_{x_i}\left(V\mid x_i\right)\right)\approx\frac{1}{2n}\left(V_A^TV_A+V_{AB^i}^TV_{AB^i}-2V_A^TV_{AB^i}\right)$$

$$Var\left(V\right)=Var\left(\left[V_A\quad V_B\right]\right)$$

x_{-i} is the remaining variable with x_i removed; $E_{x_{-i}}\left(V\mid x_i\right)$ is a series of fixed values for x_i, with x_{-i} taken multiple times over a range of variation at each fixed value, to find the mean of these outputs V; $Var_{x_i}\left(E_{x_{-i}}\left(V\mid x_i\right)\right)$ seeks the variance of $E_{x_{-i}}\left(V\mid x_i\right)$; $Var_{x_i}\left(V\mid x_i\right)$ is a series of fixed values for x_i, with x_{-i} taken multiple times over a range of variation at each fixed value, to find the variance; and $E_{x_{-i}}\left(Var_{x_i}\left(V\mid x_i\right)\right)$ seeks the mean of $Var_{x_i}\left(V\mid x_i\right)$.

The greater the value of the first-order sensitivity indicator S_{x_i}, the greater

the effect of the univariate x_i on the output response of the system. The full effect indicator $S_{x_i}^T$ has the following role: contains the first-order sensitivity of the variable x_i; also contains the effect of the interaction between x_i and other variables on the output response, and the greater the difference between its value and the first-order sensitivity indicator, the more pronounced the interaction.

The histograms of the first-order sensitivity and the sensitivity of the full effects metrics for each structural parameter are shown in **Figure 6(a)**, and the difference between these two metrics is shown in **Figure 6(b)**. Through the sensitivity analysis of these structural parameters, it is found that the first-order sensitivity of the torsional stiffness of strut, the caster length and the vertical force are greater than the other two structural parameters, and the difference between the same first-order sensitivity index and the full effect index is also greater. Therefore, the above three structural parameters have a greater influence on the critical velocity of shimmy, and the optimization of structural parameters needs to focus on the torsional stiffness of strut, the caster length and the vertical force.

4. Validation of Results

In order to verify the above results, the nonlinear shimmy model of the nose landing gear is simplified into a linear model for processing, and the influence law of the relevant structural parameters on the stability of the nose landing gear is kept constant.

Express the above nonlinear restoring force of the tire F_n expression as a segmented function:

$$F_n = \begin{cases} C_{F_\eta} F_Z \eta & |\eta| \le \eta_F \\ C_{F_\eta} F_Z \eta_F \, sign(\eta) & |\eta| \ge \eta_F \end{cases} \tag{19}$$

When small torsional displacements of the landing gear structure are considered, the nonlinear restoring force of the tire F_n and self-aligning moment M_n can be reduced to a function of the Vertical force proportional to the corresponding coefficients.

$$\begin{cases} F_n = C_{F_\eta} F_Z \eta \\ M_n = C_{M_\eta} F_Z \eta \end{cases} \tag{20}$$

Therefore, the set of equations for the nonlinear dynamics of the nose landing gear shimmy can be represented by a linear set of state equations:

$$x_1 = \theta, x_2 = \dot{\theta}, x_3 = \Delta$$

$$\begin{cases} \dot{x}_1 = x_2, \\ \dot{x}_2 = \left(-K_\theta x_1 - C_\theta x_2 - \left(L_{eff} C_{F_\eta} + C_{M_\eta} \right) F_Z \dfrac{x_3}{\sigma} \cos(\delta) - \dfrac{K}{V} \cos(\delta) x_2 \right) \Big/ I_Z, \\ \dot{x}_3 = -V/\sigma \, x_3 + V \cos(\delta) x_1 + \left(L_{eff} - a \right) \cos(\delta) x_2, \end{cases} \tag{21}$$

The system of linear equations of state is changed to matrix form A, and the frequency of the nose landing gear shimmy is found by finding the imaginary

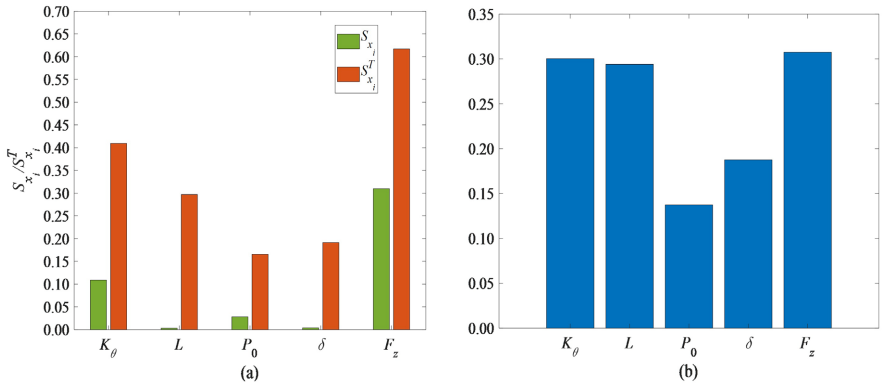

Figure 6. Sensitivity index of each structural parameter.

part of the complex eigenvalues of the matrix. **Figure 7** depicts the strut torsional vibration frequency corresponding to a change in speed. At low speeds, the effect of velocity on the vibration frequency is extremely significant, and the change in vibration frequency becomes relatively flat near the takeoff speed.

$$D=\begin{bmatrix} 0 & 1 & 0 \\ -K_\theta & -\left(C_\theta+\dfrac{K}{V}\cos(\delta)\right)\Big/I_Z & -\dfrac{\left(L_{eff}C_{F_\eta}+C_{M_\eta}\right)F_Z\cos(\delta)}{\sigma I_Z} \\ V\cos(\delta) & \left(L_{eff}-a\right)\cos(\delta) & -V/\sigma \end{bmatrix} \tag{22}$$

The Routh-Huritz criterion is used to solve for the critical velocity of the nose landing gear shimmy. Firstly, the characteristic Equation (23) is derived from the system of linear Equation (22), and the characteristic equation is written in the form of a polynomial (24), and secondly, the Routh array of Equation (24) is written as shown in **Table 3**.

$$\begin{vmatrix} I_Z s^2+K_\theta+C_\theta s+\dfrac{K}{V}s\cos(\delta) & \left(L_{eff}C_{F_\eta}+C_{M_\eta}\right)\dfrac{F_Z}{\sigma}\cos(\delta) \\ -V\cos(\delta)-\left(L_{eff}-a\right)\cos(\delta)s & s+\dfrac{V}{\sigma} \end{vmatrix}=0 \tag{23}$$

$$a_3s^3+a_2s^2+a_1s+a_0=0 \tag{24}$$

where the coefficients are given by

$$a_3=I_Z$$

$$a_2=\frac{I_ZV^2+C_\theta\sigma V+\sigma K\cos(\delta)}{V\sigma}$$

$$a_1=\frac{C_\theta V+K_\theta\sigma+K\cos(\delta)+\left(-F_ZC_{M_\eta}a+F_ZL_{eff}^2C_{F_\eta}+F_ZL_{eff}C_{M_\eta}-F_ZL_{eff}C_{F_\eta}a\right)\cos(\delta)^2}{\sigma}$$

$$a_0=\frac{K_\theta V+\left(F_ZVC_{M_\eta}+F_ZL_{eff}C_{F_\eta}V\right)\cos(\delta)^2}{\sigma}$$

According to the Ross criterion, the nose landing gear shimmy system is stable if the first column of the Ross array is all positive. **Figure 8** depicts the effect

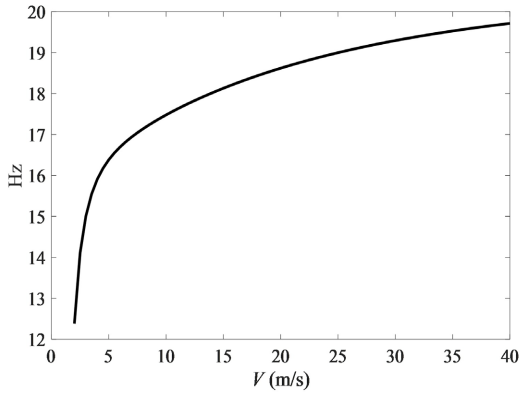

Figure 7. Frequency of torsional vibration of struts.

Table 3. Ross array of characteristic polynomials.

	First column	Second column
s^3	a_3	a_1
s^2	a_2	a_0
s^1	$\frac{a_1a_2 - a_3a_0}{a_2}$	0
s^0	a_0	0

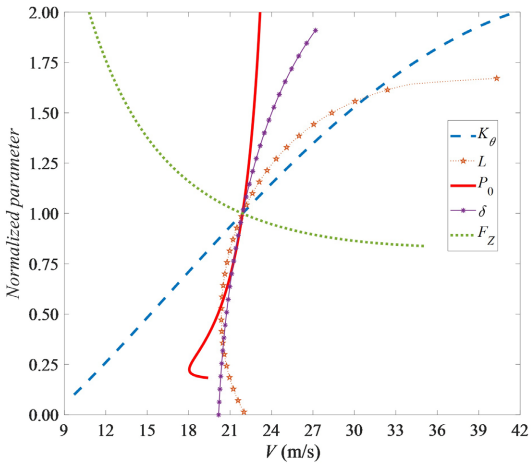

Figure 8. Influence of nose landing gear structural parameters on shimmy.

of Torsional stiffness of strut, Caster length, Rated initial tire inflation pressure, Rake angle, and Vertical force on the critical velocity of the nose landing gear Critical speed of shimmy, based on the reference case (Table 1).

There are three nose landing gear structural parameters that have a significant effect on shimmy: strut torsional stiffness, Torsional stiffness of strut, Caster length and Vertical force. As the torsional stiffness of strut increases the critical velocities of shimmy increase rapidly, from 9.7 m/s at the beginning to 41.1 m/s. The effect of the Caster length on the critical velocity of shimmy is a small de-

crease followed by a sharp increase, but the magnitude of the uncontrolled increase negatively affects the forces on the nose landing gear and the turning of the wheels. The increase of vertical force will greatly reduce the velocity of the shimmy, which has a great impact on the take-off and landing of the aircraft. When the rated initial inflation pressure of the tire is very small, the critical velocity of the shimmy will be reduced, and the effect of increasing the inflation pressure near the rated inflation pressure of the tire is very small. With the increase of the rake angle, the critical velocity of the shimmy also increases gradually. Compared with the other four structural parameters, the overall rate of change is relatively stable and gentle.

Through the above analysis, the reliability of Sobol index method to judge the influence of structural parameters on the critical velocity of nose landing gear shimmy is verified.

5. Conclusions

In this paper, a nonlinear shimmy model of landing gear is established. The influence of structural parameters related to the nose landing gear of light aircraft on the shimmy stability is analyzed. The main conclusions are as follows:

The velocity of the aircraft can affect the vibration frequency of the shimmy. At low velocity, the influence of velocity on the vibration frequency is very large.

The Sobol index method is in good agreement with the Routh-Huritz criterion to analyze the influence of structural parameters on the stability region of the nose landing gear. The torsional stiffness of strut is positively correlated with the critical velocity of the shimmy, while the vertical force is negatively correlated. The larger caster length can greatly increase the critical shimmy velocity, but it also has negative effects (such as wheel turning). Rated initial tire inflation pressure and rake angle relative to the first three parameters, the impact is small.

In future work, the Sobol index method can be used to analyze the parameters that have a large impact on the shimmy. It can save the analysis time of each parameter and improve the optimization efficiency.

Acknowledgements

This work is supported by the National Nature and Science Foundation of China under Grant No. 12072140, Natural Science Foundation of Jiangxi Province of China under Grant No. 20202ACBL201003.

Conflicts of Interest

The authors declare no conflicts of interest regarding the publication of this paper.

References

[1] Moreland, W.J. (1954) The Story of Shimmy. *Journal of the Aeronautical Sciences*, **21**, 793-808. https://doi.org/10.2514/8.3227

[2] Smiley, R.F. (1957) Correlation, Evaluation, and Extension of Linearized Theories for Tire Motion and Wheel Shimmy. NACA-TR-1299.

[3] Boekh (1954) Determination of the Elastic Constants of Airplane Tires. Technical Report Archive and Image Library.

[4] Besselink, I.J.M, Schmeitz, A.J.C. and Pacejka, H.B. (2010) An Improved Magic Formula/Swift Tyre Model that Can Handle Inflation Pressure Changes. *Vehicle System Dynamics*, **48**, 337-352. https://doi.org/10.1080/00423111003748088

[5] Thota, P., Krauskopf, B. and Lowenberg, M. (2010) Influence of Tire Inflation Pressure on Nose Landing Gear Shimmy. *Journal of Aircraft*, **47**, 1697-1706. https://doi.org/10.2514/1.C000248

[6] Ran, S., Besselink, I.J.M. and Nijmeijer, H. (2014) Application of Nonlinear Tyre Models to Analyse Shimmy. *Vehicle System Dynamics*, **52**, 387-404. https://doi.org/10.1080/00423114.2014.901542

[7] Sateesh, B. and Maiti, D.K. (2010) Vibration Control of an Aircraft Nose Landing Gear Due to Ground-Induced Excitation. *Journal of Aerospace Engineering*, **224**, 245-258. https://doi.org/10.1243/09544100JAERO661

[8] Sura, N.K. and Suryanarayan, S. (2007) Closed Form Analytical Solution for the Shimmy Instability of Nose-Wheel Landing Gears. *Journal of Aircraft*, **44**, 1985-1995. https://doi.org/10.2514/1.28826

[9] Chuban, V.D. (2019) Shimmy Analysis of Aircraft Multi-Wheel Landing Gear. *TsAGI Science Journal*, **50**, 195-209. https://doi.org/10.1615/TsAGISciJ.2019030563

[10] Somieski, G. (1997) Shimmy Analysis of a Simple Aircraft Nose Landing Gear Model Using Different Mathematical Methods. *Aerospace Science and Technology*, **1**, 545-555. https://doi.org/10.1016/S1270-9638(97)90003-1

[11] Thota, P., Krauskopf, B. and Lowenberg, M. (2009) Interaction of Torsion and Lateral Bending in Aircraft Nose Landing Gear Shimmy. *Nonlinear Dynamics*, **57**, 455-467.https://doi.org/10.1007/s11071-008-9455-y

[12] Thota, P, Krauskopf, B. and Lowenberg, M. (2010) Bifurcation Analysis of Nose Landing Gear Shimmy with Lateral and Longitudinal Bending. *Journal of Aircraft*, **47**, 87-95. https://doi.org/10.2514/1.43507

[13] Rahmani, M. and Behdinan, K. (2019) On the Effectiveness of Shimmy Dampers in Stabilizing Nose Landing Gears. *Aerospace Science and Technology*, **91**, 272-286. https://doi.org/10.1016/j.ast.2019.05.040

[14] Collins, R.L. and Black, R.J. (1969) Tire Parameters for Landing-Gear Shimmy Studies. *Journal of Aircraft*, **6**, 252-258. https://doi.org/10.2514/3.44044

[15] Behdinan, K. and Rahmani, M. (2020) Interaction of Torque Link Freeplay and Coulomb Friction Nonlinearities in Nose Landing Gear Shimmy Scenarios. *International Journal of Non-Linear Mechanics*, **119**, Article ID: 103338. https://doi.org/10.1016/j.ijnonlinmec.2019.103338

[16] Howcroft, C., Krauskopf, B., Lowenberg M.H., *et al.* (2013) Effects of Freeplay on Dynamic Stability of an Aircraft Main Landing Gear. *Journal of Aircraft*, **50**, 1908-1922. https://doi.org/10.2514/1.C032316

[17] Kewley, S., Lowenberg, M., Neild, S., *et al.* (2016) Investigation into the Interaction of Nose Landing Gear and Fuselage Dynamics. *Journal of Aircraft*, **53**, 881-891. https://doi.org/10.2514/1.C033320

[18] Thota, P., Krauskopf, B. and Lowenberg, M. (2010) Multi-Parameter Bifurcation Study of Shimmy Oscillations in a Dual-Wheel Aircraft Nose Landing Gear. *Nonlinear Dynamics*, **70**, 1675-1688. https://doi.org/10.1007/s11071-012-0565-1

[19] Jiang, Y., Feng, G., *et al.* (2023) Effect of Coulomb Friction on Shimmy of Nose Landing Gear under Time-Varying Load. *Tribology International*, **188**, Article ID: 108828. https://doi.org/10.1016/j.triboint.2023.108828